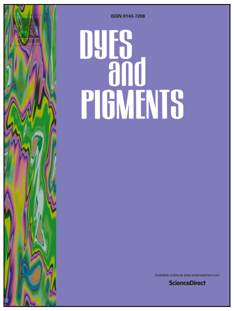

Bis-cyclometalated Ir(III) complexes with a diphenylamino group: Design, synthesis, and application in oxygen sensing

Chun Liu, Hongcui Yu, Xiaofeng Rao, Xin Lv, Zilin Jin, Jieshan Qiu

PII: S0143-7208(16)30469-7
DOI: 10.1016/j.dyepig.2016.09.022
Reference: DYPI 5474

To appear in: *Dyes and Pigments*

Received Date: 16 August 2016
Revised Date: 9 September 2016
Accepted Date: 11 September 2016

Please cite this article as: Liu C, Yu H, Rao X, Lv X, Jin Z, Qiu J, Bis-cyclometalated Ir(III) complexes with a diphenylamino group: Design, synthesis, and application in oxygen sensing, *Dyes and Pigments* (2016), doi: 10.1016/j.dyepig.2016.09.022.

Bis-cyclometalated Ir(III) complexes with a diphenylamino group: design, synthesis, and application in oxygen sensing

Chun Liu*, Hongcui Yu, Xiaofeng Rao, Xin Lv, Zilin Jin and Jieshan Qiu

[*] Dr. C. Liu, Corresponding Author
State Key Laboratory of Fine Chemicals, Dalian University of Technology, Linggong
Road 2, Dalian 116024, China.
Tel.: +86-411-84986182.
E-mail: cliu@dlut.edu.cn

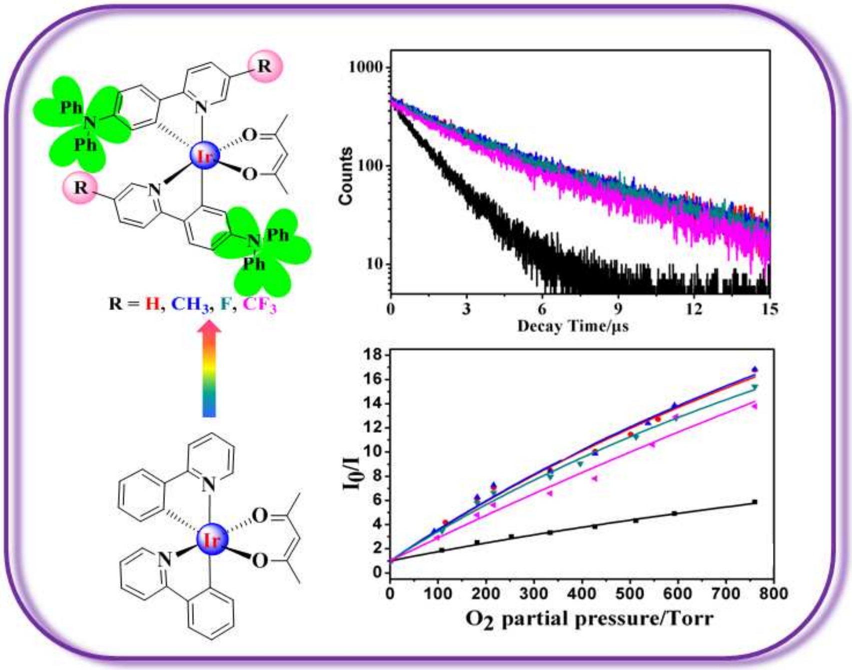

Bis-cyclometalated Ir(III) complexes with a diphenylamino group: design, synthesis, and application in oxygen sensing

Chun Liu*, Hongcui Yu, Xiaofeng Rao, Xin Lv, Zilin Jin and Jieshan Qiu

[*] Dr. C. Liu, Corresponding-Author

State Key Laboratory of Fine Chemicals, Dalian University of Technology, Linggong Road 2, Dalian 116024, China

Tel.: +86-411-84986182.

E-mail: cliu@dlut.edu.cn

Abstract:

A series of C^N type bis-cyclometalated Ir(III) complexes (**Ir1-Ir4**) with a diphenylamino group at the 4-position of the phenyl ring of 2-phenylpyridine (ppy) have been prepared and fully characterized. The influences of substituents (-H, $-CH_3$, -F, $-CF_3$) at the pyridyl moiety of ppy on the photophysical and electrochemical properties of these Ir(III) complexes have been investigated systematically by comparison with the model complex $Ir(ppy)_2(acac)$. The Ir(III) complexes (**Ir1-Ir4**) show phosphorescence with emission maxima in the range of 530–558 nm, which are all red-shifted relative to $Ir(ppy)_2(acac)$ (λ_{max} = 518 nm). These Ir(III) complexes demonstrate longer phosphorescence lifetimes and better oxygen-sensitivity than $Ir(ppy)_2(acac)$. It is remarkable that introduction of both diphenylamino and trifluoromethyl groups into the cyclometalating ligand enhances the photostability of the corresponding Ir(III) complexes efficiently. The results reveal that the bulky and electron-donating characteristics of the diphenylamino group enhance the performances of the Ir(III) complexes in oxygen sensing.

Keywords: *Ir(III) complex, diphenylamino group, phosphorescence lifetime, oxygen sensing, photostability*

1. Introduction

Oxygen sensors have important applications in various fields, including clinical analysis, environmental monitoring, and food packaging [1-6]. An optical oxygen sensor relies on the quenching of the luminescence of an oxygen-sensitive probe (OSP) by molecular oxygen [7, 8]. To reach smooth oxygen diffusion and minimize probe self-quenching, OSPs are usually doped into an appropriate matrix (such as a polymer) [9, 10]. Reversibility and long-term stability are important factors to influence the overall performances of the sensor. However, due to the photo-bleaching nature of indicator, OSPs immobilized in supporting matrices usually demonstrate decreased intensity (poor photostability) during the illumination period under continuous conditions [11, 12]. Therefore, the development of novel OSPs with enhanced photostability is crucial to an efficient oxygen sensor. At present, most oxygen-sensitive probes (OSPs) are based on heavy metal complexes such as ruthenium(II), platinum(II), iridium(III), and so on [13-15]. The high coupling of the iridium metal core (spin-orbit coupling constant $\zeta_{Ir} = 3909$ removes the spin-forbidden nature of the radiative relaxation of the triplet state and demonstrates high phosphorescence efficiencies [16, 17]. The facile tunability of cyclometalated Ir(III) complexes by the coordinating ligands differentiates them from other organometallic compounds [18, 19]. The unique properties of Ir(III) complexes make these compounds particularly suitable for applications in oxygen sensing [20, 21]. However, it is still a challenge to enhance the photostability of cyclometalated Ir(III) complexes and increase their oxygen sensitivity as luminescent O_2-sensing materials.

Electron-donating diphenylamino group (-NPh_2) has been often used in numerous organic electroluminescence materials, owing to the good hole-transporting capability as well as the bulky size for suppressing a self-quenching process [22-24]. However, there have been only a few complexes modified with a diphenylamino group used in oxygen sensing. In 2009, Chan and co-workers [25] reported the use of Ir(ppy-NPh_2)$_3$ for luminescence oxygen sensing. Due to the larger dynamic range of response and higher sensitivity, this complex represents a promising candidate for oxygen sensing in contrast to Ir(ppy)$_3$. By chemically manipulating the Pt(ppy)$_2$(acac) with a diphenylamino group on the phenyl ring of ppy, a new family of cyclometalated Pt(II) complexes with long phosphorescence lifetimes and good oxygen sensing properties have been reported by our group [26]. Inspired by these reports, we envision that bis-cyclometalated Ir(III) complexes bearing one acetylacetonate and two 2-phenylpyridine (ppy) ligands functionalized with a bulky electron-donating diphenylamino group could also serve as efficient OSPs for oxygen-sensing. In this paper, we present the synthesis and characterization of a series of Ir(III) complexes (**Ir1-Ir4**) functionalized with a diphenylamino group at the cyclometalating ligands and a acetylacetone (acac) as the ancillary ligand. The photophysical and electrochemical properties of these bis-cyclometalated Ir(III) complexes have been investigated systematically, and the results demonstrate that introduction of a diphenylamino group at the 4-position of phenyl ring in ppy can improve the photostability of the Ir(III) complexes effectively compared with Ir(ppy)$_2$(acac). Introducing a -CF$_3$ group at the 5-position of the pyridyl ring of cyclometalating ligand could further improve the photostability. These photostable Ir(III) complexes with prolonged phosphorescence lifetimes exhibit efficient oxygen-sensitivity compared with Ir(ppy)$_2$(acac).

2. Experimental

2.1. Materials and measurements

All starting materials were purchased from commercial suppliers and used without further purification. The solvents were treated as required prior to use. ^{1}H NMR and ^{13}C NMR spectra were recorded on a 400 MHz Varian Unity Inova spectrophotometer. Mass spectra were recorded with a MALDI micro MX spectrometer. UV/Vis absorption spectra were recorded on an HP8453 UV/Vis spectrophotometer. Emission spectra were recorded with a PTI-700 spectrofluorimeter. Photoluminescence quantum yields were measured relative to [Ir(ppy)$_2$(acac)] (Φ_P = 0.34 in CH$_2$Cl$_2$, under degassed conditions). Phosphorescence lifetimes were measured on an Edinburgh FLS920 Spectrometer (picosecond pulsed diode laser made in the U. K., model: EPL-405). Cyclic voltammograms of the Ir(III) complexes were recorded on an electrochemical workstation (BAS100B/W, USA) at room temperature in a

0.1 M $[Bu_4N]PF_6$ solution under argon conditions. Phosphorescent intensity response of sensing films of the Ir(III) complexes were recorded with a F-7000 spectrofluorimeter. Thickness of sensing films was analyzed on a QUANTA 450 scanning electron microscopy (SEM).

2.2. Synthesis

Here Scheme 1. Synthesis of bis-cyclometalated Ir(III) complexes for this study. (i) $Pd(OAc)_2$, K_2CO_3, $EtOH/H_2O$ 3:1(v/v), 80 ºC, in air, 30-60 min. (ii) $IrCl_3\cdot 3H_2O$, $EtOCH_2CH_2OH/H_2O$ 3:1(v/v), 110 ºC, N_2, 24 h. (iii) Hacac, K_2CO_3, $EtOCH_2CH_2OH$, 120 ºC, N_2, 24 h.

Chemical structures and the detailed synthetic protocols of the Ir(III) complexes are shown in Scheme 1. The cyclometalating ligands **L1-L4** were prepared via a palladium-catalyzed ligand-free and aerobic Suzuki reaction in aqueous ethanol developed by our group [27]. All of the bis-cyclometalated Ir(III) complexes were synthesized in two steps from the cyclometalation of $IrCl_3\cdot 3H_2O$ with the corresponding ligands to form the chloride-bridged dimers initially, followed by treatment with acetylacetone (Hacac) in the presence of K_2CO_3 to obtain the target Ir(III) complexes.

2.2.1. Synthetic procedure of ligands ***L1-L4***

A mixture of 2-pyridyl bromide, 1.5 equiv. of arylboronic acid, 2 equiv. of K_2CO_3, $Pd(OAc)_2$ (1.5 mol%), ethanol/water (3:1 v/v) was stirred at 80 °C in air for indicated time. The reaction mixture was added to brine (15 mL) and extracted with ethyl acetate (4×15 mL). The solvent was concentrated under vacuum, and the product was isolated by short-column chromatography on silica gel.

2.2.2. Synthetic procedure of Ir(III) complexes ***Ir1-Ir4***

A mixture of $IrCl_3 \cdot 3H_2O$ (0.5 mmol) and 2.5 equiv. of cyclometalating ligand was heated to 110 °C in a mixed solvent of 2-ethoxyethanol and water (3:1 v/v) under nitrogen for 24 h. Upon cooling to room temperature, the yellow precipitate was collected by filtration and washed with water. The wet solid was completely dried to give the crude cyclometalated Ir(III) μ-chloro-bridged dimer. Without further purification, the dimeric Ir(III) complex, subsequently reacted with 10 equiv. of the acetylacetone (Hacac) in the presence of 10 equiv. of K_2CO_3 in 2-ethoxyethanol at 120 °C under nitrogen for 24 h. After cooling to room temperature, the precipitate was collected by filtration, washed with water and dried. The crude product was purified by column chromatography over silica using CH_2Cl_2:*n*-hexane (1:1) as eluent to provide the desired Ir(III) complexes.

Ir1: Yield 57%, a yellow solid; ^{1}H NMR (400 MHz, $CDCl_3$) δ = 8.24 (d, *J* = 4.8 Hz, 2H), 7.42-7.36 (m, 4H), 7.30 (d, *J* = 8.0 Hz, 2H), 7.13 (t, *J* = 8.0 Hz, 8H), 6.95-6.90 (m, 12H), 6.79 (t, *J* = 6.8 Hz, 2H), 6.48 (d, *J* = 8.0 Hz, 2H), 5.77 (s, 2H), 5.23 (s, 1H), 1.82 (s, 6H).

Ir2: Yield 48%, a yellow solid; ^{1}H NMR (400 MHz, $CDCl_3$) δ = 8.04 (m, 2H), 7.31 (d, *J* = 8.0 Hz, 2H), 7.26-7.24 (m, 2H), 7.19 (d, *J* = 7.2 Hz, 2H), 7.12 (t, *J* = 8.0 Hz, 8H), 6.92 (d, *J* = 8.0 Hz, 12H), 6.49 (m, 2H), 5.72 (d, *J* = 2.4 Hz, 2H), 5.22 (s, 1H), 2.20 (s, 6H), 1.82(s, 6H). ^{13}C NMR (100 MHz, $CDCl_3$) δ = 184.3, 165.2, 147.6, 147.3, 147.0, 146.9, 138.9, 136.9, 129.6, 128.7, 125.9, 125.0, 123.7, 122.3, 117.4, 114.3, 100.4, 28.9, 18.4. MALDI-TOF-MS (m/z): 962.3136 $[M]^+$, 863.2747 $[M\text{-acac}]^+$.

Ir3: Yield 50%, a greenish-yellow solid; ^{1}H NMR (400 MHz, $CDCl_3$) δ = 8.10 (t, *J* = 2.4 Hz, 2H), 7.39-7.36 (m, 2H), 7.23 (d, *J* = 8.0 Hz, 2H), 7.20-7.13 (m, 10H), 6.97-6.92 (m, 12H), 6.50 (d, *J* = 8.0 Hz, 2H), 5.69 (d, *J* = 2.4 Hz, 2H), 5.26 (m, 1H), 1.84 (s, 6H). ^{13}C NMR (100 MHz, $CDCl_3$) δ = 184.9, 164.7, 157.8, 155.3, 147.5, 147.3, 146.5, 137.1, 135.6, 128.8, 125.3, 125.2, 124.2, 123.9, 123.7, 122.8, 118.2, 118.1, 114.1, 100.7, 28.8. MALDI-TOF-MS (*m/z*): 970.2690 $[M]^+$, 871.2173 $[M\text{-acac}]^+$.

Ir4: Yield 69%, an orange-yellow solid; ^{1}H NMR (400 MHz, $CDCl_3$) δ = 8.42 (s, 2H), 7.51-7.45 (m, 4H), 7.32 (d, *J* = 8.0 Hz, 2H), 7.18-7.14 (m, 8H), 7.01-6.95 (m, 12H), 6.54-6.51 (m, 2H), 5.63 (d, *J* = 2.4 Hz, 2H), 5.26 (s, 1H), 1.83 (s, 6H). ^{13}C NMR (100 MHz, $CDCl_3$) δ = 185.2, 171.0, 150.0, 149.0, 146.8, 144.7, 135.5, 133.2, 133.1, 129.0, 126.1, 125.9, 124.3, 123.8, 123.6, 122.2, 121.8, 121.6, 117.0, 113.2, 100.9, 28.7. MALDI-TOF-MS (*m/z*): 1070.2633 $[M]^+$, 971.2294 $[M\text{-acac}]^+$.

2.3. Preparation of oxygen sensing films and their photostability

Oxygen sensing films were prepared according to the literature [28]: EC (9.95 mg) was dissolved in CH_2Cl_2 (0.90 mL) and then 0.10 mL **Ir1** (0.5 mg/mL) in CH_2Cl_2 was added to the solution. After thoroughly mixing, 0.1

mL of the solution was coated on a silica glass disk (diameter 1.4 cm). The solvent was evaporated at room temperature and a thin film was obtained as shown in Fig. 4(A). The samples with different loading levels and different matrices were prepared with procedure similar to that described above. The photostability of the complexes in EC film was investigated by illuminating the sensing film with a 254 nm 16 W ZF-7A UV lamp at a distance of 3 cm in the air for 90 min. Emission intensities were measured before and after exposure of the film to illumination. The power density on the films is 21.5 W/m^2. General procedure for the oxygen sensing test was performed according to the reported method [29].

3. Results and Discussion

3.1. Photophysical and electrochemical properties

UV−vis absorption spectra and emission spectra of complexes **Ir1-Ir4** in CH_2Cl_2 (1.0×10^{-5} M) at room temperature are presented in Fig. 1 and the corresponding data are listed in Table 1. Similarly to other previously reported cyclometalated Ir(III) complexes [30, 31], the complexes (**Ir1-Ir4**) exhibit strong absorption bands in the ultraviolet region belong to the spin-allowed intraligand ($^1\pi-\pi^*$) transitions. The long wavelength with lower extinction coefficient can be assigned to singlet and triplet metal-to-ligand charge-transfer (^{1}MLCT and ^{3}MLCT) transitions. The results in Fig. 1 show that **Ir1-Ir4** functionalized with an electron-donating diphenylamino group have larger molar extinction coefficient than that of $Ir(ppy)_2(acac)$. Especially, the spectrum of **Ir4** is red-shifted obviously compared to other complexes under the same measurement conditions, due to the electron-withdrawing ability of the -CF_3 substituent [32, 33].

The normalized emission spectra of these complexes are shown in Fig. 1. The emission maxima of **Ir1-Ir4** are red-shifted compared to $Ir(ppy)_2(acac)$ (λ_{max} at 518 nm), owing to the electron-donating ability of the diphenylamino moiety. Additionally, the substituents at 5-position of pyridyl ring also affected the emission properties of the complexes. Introducing a -CH_3 group at the 5-position of the pyridyl ring results in a slight blue-shift of 2 nm for **Ir2** (λ_{max} at 530 nm) relative to **Ir1** (λ_{max} at 532 nm). Instead of a -CH_3 group with a fluorine, a red-shift of 4 nm for **Ir3** is reached, while introducing a -CF_3 group at the same position imparts a more substantial red-shift up to 26 nm for **Ir4** (λ_{max} at 558 nm). These results show that the emission of the complexes could be finely tuned by the modification of the structures of complexes. The phosphorescence quantum yields (Φ_p) of **Ir1-Ir4** range from 0.18 to 0.30 (Table 1). The phosphorescence lifetimes (τ) of **Ir1-Ir4** in degassed CH_2Cl_2 are in the range of 3.46-3.90 μs at room temperature (Fig. 2), which are longer than that of $Ir(ppy)_2(acac)$ (1.55 μs).

The electrochemical properties of the Ir(III) complexes were studied by cyclic voltammetry (CV) and the results are also listed in Table 1. The HOMO and LUMO energies can be calculated by following equations (E_{HOMO} (eV) = -e(4.4 +E_{ox}^{onset}), E_{LUMO} (eV)= E_{HOMO} + E_g). The energy gaps (E_g) between the HOMO and LUMO levels of **Ir1-Ir4** (2.47, 2.49, 2.43 and 2.36 eV) decrease in comparison with the $Ir(ppy)_2(acac)$ (2.54 eV). At an anodic scan rate of 100 mV/s, the CVs of **Ir1-Ir4** show oxidation potentials of 0.63, 0.58, 0.68, and 0.77 V versus saturated calomel electrode (SCE), respectively (see Fig. S2, Supplementary Information). These positive oxidation potentials are assigned to the metal-centered Ir(III)/Ir(IV) oxidation couple, in accordance with the reported cyclometalated Ir(III) systems [34]. As shown in Table 1, it is found that introducing the electron-donating group -CH_3 in the pyridine unit leads to a low potential for **Ir2**, while introducing an electron-withdrawing group -F (**Ir3**) or -CF_3 (**Ir4**) at the same position makes the oxidation process shift to a more positive potential.

Here Fig. 1. Absorption (up) and emission spectra (down, λ_{ex}= 400 nm) of **Ir1-Ir4** and $Ir(ppy)_2(acac)$ in CH_2Cl_2 solution at room temperature.

Here Fig. 2. Phosphorescence decay profiles of **Ir1-Ir4** and $Ir(ppy)_2(acac)$ in CH_2Cl_2 solution at room temperature.

Here Table 1. Photophysical and electrochemical data of the Ir(III) complexes.

3.2. Fitting Formula of Oxygen Sensing

Optical oxygen sensing process of the luminescence quenching involves dynamic collision between molecular oxygen (triplet) and the excited state of the OSPs, leading to a reduction of its intensity and decay time [10]. The process can be described as follows: $Ir^{III}*+O_2 \rightarrow Ir^{III}+O_2*$, where Ir^{III} denotes the complex and the “*” indicates the excited state (Fig. 3) [35, 36]. The phosphorescence intensity of Ir(III) complexes immobilized in a matrix is quenched by oxygen according to the

Stern-Volmer equation [37-39]:

$$\frac{I_0}{I} = \frac{\tau_0}{\tau} = 1 + K_{\mathrm{SV}} \cdot p_{\mathrm{O_2}} \qquad (1)$$

In the equation, I is the phosphorescence intensity, and τ is the lifetime of an OSP. I_0 and τ_0 are the corresponding values in the absence of oxygen. K_{SV} is the Stern-Volmer quenching constant and $p_{\mathrm{O_2}}$ is the partial pressure of oxygen. For heterogeneous O_2-sensing films, a two-site model is required to study the quenching effect. In the two-site model, the O_2-sensitive complexes are considered as two different portions. In the conventional form, it reads as follows (see Eqs 2 and 3) [40, 41].

$$\frac{I}{I_0} = \frac{\tau}{\tau_0} = \frac{f_1}{1+K_{\mathrm{SV1}} \cdot p_{\mathrm{O_2}}} + \frac{f_2}{1+K_{\mathrm{SV2}} \cdot p_{\mathrm{O_2}}} \qquad (2)$$

$$f_1 + f_2 = 1 \qquad (3)$$

where f_1 and f_2 denote the fractional contribution of the total luminescence emission from the OSP due to the heterogeneity of the microenvironment. It is assumed that there exists two distinctly different components, one (f_1) being quenchable, the other (f_2) either not being quenched at all, or being quenched at a very different rate. The weighted quenching constant K_{sv}^{app} ($K_{SV}^{app} = f_1 \cdot K_{SV1} + f_2 \cdot K_{SV2}$) is the guide of the sensitivity of an oxygen sensor, and higher values of K_{sv}^{app} indicate that the oxygen sensor is more sensitive to oxygen quenching.

Here Fig. 3. Illustration of simplified mechanism for oxygen sensing.

3.3. Effects of the polymer matrices and OSP contents on oxygen sensing

An optical oxygen sensor is ususally composed of an OPS and a sensor matrix. Generally, polymers or organically modified silica (ormosils) are mainly employed as matrix materials in an optical oxygen sensor [25, 42-45]. The selection of a favorable matrix is a key to a successful sensor [10]. In this work, we prepared sensing films of OSPs immobilized in ethyl cellulose (EC), polystyrene (PS), poly(ether-ketone-ketone) (PPEK), poly(cyclohexene carbonate) (PCHC) and IMPES-C , respectively (see Fig. S3, Supplementary Information). The results in Table S1 demonstrate that the weighted quenching constant K_{SV}^{app} of **Ir1** incorporated into EC is higher than those of others. This is contributed to the large permeability coefficient of EC, providing good permeability to oxygen [25, 46]. In addition, it is known that the OSP contents strongly affect the quenching efficiency, the sensitivity and linearity as well as the response time of an oxygen sensor [17, 47]. The detailed oxygen sensing properties of **Ir1**/EC with different **Ir1** loadings are presented in Table S2. It is found that the optimum weight content of **Ir1** immobilized in EC is 0.5 wt%, which is consistent with the previous result [48]. The reason for this might be that at this content the polymer matrix protects the OSPs from potential interference and avoids self-quenching efficiently in this sensor system. Additionally, the thickness of the oxygen sensing film at the optimum weight content has been characterized by a QUANTA 450 scanning electron microscopy (SEM). The SEM micrograph shows that the thickness of the oxygen sensing film is ca. 4.7 μm (Fig. 4).

Here Fig. 4. (A) The transparent quartz plate (*r* = 7.0 mm) whose inner surface is covered with the oxygen sensing film. (B) SEM micrograph of the oxygen sensing film. (C) The diagram of the sensing layer.

3.4. Photostability of oxygen sensing films

An ideal oxygen sensor should possess high photostability to construct robust oxygen sensing systems, which is critical to long-term sensing reliability. The following study was conducted to identify the sensor's photostability for Ir(III) complexes immobilized on EC against continuous irradiation with a 254 nm UV lamp under air atmosphere. After 90 min of irradiation, the emission intensity of the sensing films reduced in different degrees (Fig. 5). The photostabilities of **Ir1-Ir4** are obviously higher than that of the reference complex Ir(ppy)$_2$(acac). In fact, 55%, 58%, 52% and 43% decreases in intensity of **Ir1-Ir4** are observed compared to 79% for Ir(ppy)$_2$(acac). The photostabilities of these Ir(III) complexes are varied due to the differences in their chemical structures. It is clear that the diphenylamino group has a distinct positive effect on the photostability. Furthermore, the substituent at the pyridyl ring also affects the photostability of the Ir(III) complexes. It is observed that the complex **Ir4** with a strong electron-withdrawing -CF$_3$ group on the 5-position of the pyridyl ring is more photostable than other Ir(III) complexes. The experimental data are in good agreement with related results previously reported by our group [43, 48].

Here Fig. 5. Photo-degradation histograms for the Ir(III) complexes/EC films under continuous illumination for 90 min at ambient atmospheric conditions.

Here Table 2. Some of Ir(III) complexes used as oxygen sensing probes.

3.5. Oxygen sensing properties

In general, an oxygen sensor with the ratio of I_0/I_{100} (I_0 and I_{100} represent the detected luminescence intensities from a film exposed to 100% nitrogen and 100% oxygen, respectively) more than 3.0 is suitable for oxygen sensing [49]. The I_0/I_{100} values of previous reported sensors with Ir(III) complexes immobilized in polymer matrix are shown in Table 2 and the data can be used to evaluate the O_2 sensitivity. To compare the O_2-sensing properties of the complexes quantitatively, the O_2-sensing data of **Ir1-Ir4** and Ir(ppy)$_2$(acac) (see Fig. S4, Supplementary Information) are fitted to the two-site model, and the results are summarized in Table S3. **Ir1-Ir4** exhibit better oxygen sensitivity compared to Ir(ppy)$_2$(acac). The I_0/I_{100} values of these Ir(III) complexes immobilized in EC film are 16.2, 16.4, 15.2, 14.1 and 5.8, respectively (Table 2). It is clear that the **Ir2** immobilized in EC exhibits the highest sensitivity to O_2 (Fig. 6) at a K_{SV}^{app} value up to 0.02698 Torr^{-1} (1 Torr = 133.322 Pa), which is about 3.4 times higher than that of Ir(ppy)$_2$(acac) (0.00792 Torr^{-1}). The reason for this might be that the long-lived excited states of **Ir1-Ir4** promote the quenching pathway. This means that, per encounter with an O_2 molecule, **Ir1-Ir4** are more likely to be quenched than Ir(ppy)$_2$(acac). This may be due to the unique properties of the diphenylamino substituent, which breaks the molecular planarity of cyclometalating ligands and reduces the aggregation tendency of Ir(III) complexes. In addition, introducing substituents (-H, $-CH_3$, -F, $-CF_3$) into the pyridyl moiety of the cyclometalating ligands has relatively little influence on the sensitivity of the sensors (Fig. 6). Therefore, the diphenylamino group at the 4-position of phenyl ring of ppy is crucial to enhance the oxygen sensitivity.

Furthermore, an operational stability test was conducted by reading the luminescence intensity signals while oxygenated and deoxygenated gases were switched for 4000 s (shown in Fig. S5, Supplementary Information). All of the oxygen sensing films demonstrated good operational stability during the whole process. Additionally, fast response and recovery times were obtained. The response times of the **Ir1-Ir4** immobilized in EC are ca. 4.0 s for switching from nitrogen to oxygen, and ca. 5.0 s for switching from oxygen to nitrogen. These bis-cyclometalated Ir(III) complexes with excellent oxygen-sensing properties and stability are potential candidates for online continuous monitoring of oxygen concentrations.

Here Fig. 6. Stern-Volmer plots for oxygen sensing films of Ir(III) complexes immobilized in EC (intensity ratios I_0/I versus O_2 partial pressure).

4. Conclusions

In summary, a series of cyclometalated Ir(III) complexes bearing a bulky electron-donating diphenylamino substituent (**Ir1-Ir4**) have been synthesized and fully characterized. The results demonstrate that the diphenylamino group is an attractive substituent for tuning the photophysical and electrochemical properties of the corresponding Ir(III) complexes. The emission bands of **Ir1-Ir4** are red-shifted and phosphorescence lifetimes are prolonged relative to the unsubstituted reference Ir(ppy)$_2$(acac). Immobilized in ethyl cellulose, **Ir1-Ir4** impart favorable oxygen sensitivity and good photostability against irradiation. Especially, **Ir4** with a trifluoromethyl group at the 5-position of the pyridyl ring exhibits the highest photostability. These results might provide new insights into the chemical modification of cyclometalated Ir(III) complexes, leading to the design of oxygen sensitive probes with high performances.

Acknowledgments

The authors thank the financial support from the National Natural Science Foundation of China (21276043, 21421005), Dalian University of Technology (DUTTX2015102), and Open Fund of Key Laboratory of Biotechnology and Bioresources Utilization (Dalian Minzu University), State Ethnic Affairs Commission & Ministry of Education.

Appendix A. Supplementary data

Supplementary data related to this article can be found in the online version, at http://dx.doi.

References

[1] Sakadžić S, Roussakis E, Yaseen MA, Mandeville ET, Srinivasan VJ, Arai K, et al. Two-photon high-resolution measurement of partial pressure of oxygen in cerebral vasculature and tissue. Nat Methods 2010;7:755-9.

[2] Lehner P, Staudinger C, Borisov SM, Klimant I. Ultra-sensitive optical oxygen sensors for characterization of nearly anoxic systems. Nat Commun 2014;5:4460.

[3] Koshiba Y, Nakamura Y, Ito D, Yokoyama T, Okazaki S, Nakagawa H, et al. Development of a durable fiber-optic oxygen sensor for harsh underground environments. Talanta 2010;82:1495-9.

[4] Persson A, Gross E, Laurent P, Busch KE, Bretes H, de Bono M. Natural variation in a neural globin tunes oxygen sensing in wild Caenorhabditis elegans. Nature 2009;458:1030-3.

[5] Quaranta M, Borisov SM, Klimant I. Indicators for optical oxygen sensors. Bioanal Rev 2012;4:115-57.

[6] Mills A. Oxygen indicators and intelligent inks for packaging food. Chem Soc Rev

2005;34:1003-11.

[7] Wolfbeis OS. Materials for fluorescence-based optical chemical sensors. J Mater Chem 2005;15:2657-69.

[8] Gao R, Ho DG, Hernandez B, Selke M, Murphy D, Djurovich PI, et al. Bis-cyclometalated Ir(III) complexes as efficient singlet oxygen sensitizers. J Am Chem Soc 2002;124:14828-9.

[9] McDonagh C, Burke CS, MacCraith BD. Optical chemical sensors. Chem Rev 2008;108:400-22.

[10] Wang XD, Wolfbeis OS. Optical methods for sensing and imaging oxygen: materials, spectroscopies and applications. Chem Soc Rev 2014;43:3666-761.

[11] Lee SK, Okura I. Photostable optical oxygen sensing material: platinum tetrakis(pentafluorophenyl)porphyrin immobilized in polystyrene. Anal Commun 1997;34:185-8.

[12] Amao Y, Miyashita T, Okura I. Platinum tetrakis (pentafluorophenyl) porphyrin immobilized in polytrifluoroethylmethacrylate film as a photostable optical oxygen detection material. J Fluorine Chem 2001;107:101-6.

[13] Ji S, Wu W, Wu W, Song P, Han K, Wang Z, et al. Tuning the luminescence lifetimes of ruthenium(II) polypyridine complexes and its application in luminescent oxygen sensing. J Mater Chem 2010;20:1953-63.

[14] Wu W, Sun J, Ji S, Wu W, Zhao J, Guo H. Tuning the emissive triplet excited states of platinum(II) schiff base complexes with pyrene, and application for luminescent oxygen sensing and triplet–triplet-annihilation based upconversions. Dalton Trans 2011;40:11550-61.

[15] Huynh L, Wang Z, Yang J, Stoeva V, Lough A, Manners I, et al. Evaluation of phosphorescent rhenium and iridium complexes in polythionylphosphazene films for oxygen sensor applications. Chem Mater 2005;17:4765-73.

[16] Lowry MS, Bernhard S. Synthetically tailored excited states: phosphorescent, cyclometalated iridium(III) complexes and their applications. Chem - Eur J 2006;12:7970-7.

[17] Monti F, Baschieri A, Gualandi I, Serrano-Pérez JJ, Junquera-Hernández JM, Tonelli D, et al. Iridium(III) complexes with phenyl-tetrazoles as cyclometalating ligands. Inorg Chem 2014;53:7709-21.

[18] Costa RD, Orti E, Bolink HJ, Monti F, Accorsi G, Armaroli N. Luminescent ionic transition-metal complexes for light-emitting electrochemical cells. Angew Chem Int Ed 2012;51:8178-211.

[19] Ladouceur S, Zysman-Colman E. A comprehensive survey of cationic iridium(III) complexes bearing nontraditional ligand chelation motifs. Eur J Inorg Chem 2013:2985-3007.

[20] Borisov SM, Klimant I. Ultrabright oxygen optodes based on cyclometalated iridium(III) coumarin complexes. Anal Chem 2007;79:7501-9.

[21] Marín-Suárez M, Curchod BF, Tavernelli I, Rothlisberger U, Scopelliti R, Jung I, et al. Nanocomposites containing neutral blue emitting cyclometalated iridium(III) emitters for oxygen sensing. Chem Mater 2012;24:2330-8.

[22] Adachi C, Nagai K, Tamoto N. Molecular design of hole transport materials for obtaining high durability in organic electroluminescent diodes. Appl Phys Lett 1995;66:2679-81.

[23] Zhou G, Ho CL, Wong WY, Wang Q, Ma D, Wang L, et al. Manipulating charge-transfer character with electron-withdrawing main-group moieties for the color tuning of iridium electrophosphors. Adv Funct Mater 2008;18:499-511.

[24] Ho CL, Wong KL, Kong HK, Ho YM, Chan CT, Kwok WM, et al. A strong two-photon induced phosphorescent Golgi-specific in vitro marker based on a heteroleptic iridium complex. Chem

Commun 2012;48:2525-7.

[25] Mak CS, Pentlehner D, Stich M, Wolfbeis OS, Chan WK, Yersin H. Exceptional oxygen sensing capabilities and triplet state properties of Ir(ppy-NPh$_2$)$_3$. Chem Mater 2009;21:2173-5.

[26] Liu C, Song X, Rao X, Xing Y, Wang Z, Zhao J, et al. Novel triphenylamine-based cyclometalated platinum(II) complexes for efficient luminescent oxygen sensing. Dyes Pigm 2014;101:85–92.

[27] Liu C, Rao X, Song X, Qiu J, Jin Z. Palladium-catalyzed ligand-free and aqueous suzuki reaction for the construction of (hetero) aryl-substituted triphenylamine derivatives. RSC Adv 2013;3:526-31.

[28] Liu C, Yu H, Xing Y, Gao Z, Jin Z. Photostable ester-substituted bis-cyclometalated cationic iridium(III) complexes for continuous monitoring of oxygen. Dalton Trans 2016;45:734-41.

[29] Xing Y, Liu C, Xiu J-H, Li J-Y. Photostable fluorophenyl-substituted cyclometalated platinum(II) emitters for monitoring of molecular oxygen in real time. Inorg Chem 2015;54:7783-90.

[30] Zhou Y, Gao H, Wang X, Qi H. Electrogenerated chemiluminescence from heteroleptic iridium(III) complexes with multicolor emission. Inorg Chem 2015;54:1446-53.

[31] Lee W, Kwon TH, Kwon J, Kim JY, Lee C, Hong JI. Effect of main ligands on organic photovoltaic performance of Ir(III) complexes. New J Chem 2011;35:2557-63.

[32] Wang R, Deng L, Zhang T, Li J. Substituent effect on the photophysical properties, electrochemical properties and electroluminescence performance of orange-emitting iridium complexes. Dalton Trans 2012;41:6833-41.

[33] Ho CL, Lam CS, Sun N, Ma D, Liu L, Yu ZQ, et al. Synthesis, characterization, and electroluminescent properties of iridium(III) 2-phenylpyridine-type complexes containing trifluoromethyl substituents and various main-group moieties. Isr J Chem 2014;54:999-1014.

[34] Ho CL, Wong WY, Zhou GJ, Yao B, Xie Z, Wang L. Solution-processible multi-component cyclometalated iridium phosphors for high-efficiency orange-emitting OLEDs and their potential use as white light sources. Adv Funct Mater 2007;17:2925-36.

[35] Takizawa SY, Aboshi R, Murata S. Photooxidation of 1,5-dihydroxynaphthalene with iridium complexes as singlet oxygen sensitizers. Photochem Photobiol Sci 2011;10:895-903.

[36] Abdel-Shafi AA, Bourdelande JL, Ali SS. Photosensitized generation of singlet oxygen from rhenium(I) and iridium(III) complexes. Dalton Trans 2007;251:2510-6.

[37] Demas JN, Degraff BA, Xu W. Modeling of luminescence quenching-based sensors: comparison of multisite and nonlinear gas solubility models. Anal Chem 1995;67:1377-80.

[38] Nelissen HF, Kercher M, De Cola L, Feiters MC, Nolte RJ. Photoinduced electron transfer between metal-coordinated cyclodextrin assemblies and viologens. Chem - Eur J 2002;8:5407-14.

[39] Huynh L, Wang Z, Yang J, Stoeva V, Lough A, Ian Manners A, et al. Evaluation of phosphorescent rhenium and iridium complexes in polythionylphosphazene films for oxygen sensor applications. Chem Mater 2005;17:4756-73.

[40] Xu W, McDonough III RC, Langsdorf B, Demas J, DeGraff B. Oxygen sensors based on luminescence quenching: interactions of metal complexes with the polymer supports. Anal Chem 1994;66:4133-41.

[41] McGee KA, Mann KR. Inefficient crystal packing in chiral [Ru(phen)$_3$](PF$_6$)$_2$ enables oxygen molecule quenching of the solid-state mlct emission. J Am Chem Soc 2009;131:1896-902.

[42] Fernandez-Sanchez J, Roth T, Cannas R, Nazeeruddin MK, Spichiger S, Graetzel M, et al. Novel

oxygen sensitive complexes for optical oxygen sensing. Talanta 2007;71:242-50.

[43] Xing Y, Liu C, Song X, Li J. Photostable trifluoromethyl-substituted platinum(II) emitters for continuous monitoring of molecular oxygen. J Mater Chem C 2015;3:2166-74.

[44] Ji S, Wu W, Wu Y, Zhao T, Zhou F, Yang Y, et al. Real-time monitoring of luminescent lifetime changes of PtOEP oxygen sensing film with LED/photodiode-based time-domain lifetime device. Analyst 2009;134:958-65.

[45] Tripathi VS, Lakshminarayana G, Nogami M. Optical oxygen sensors based on platinum porphyrin dyes encapsulated in ormosils. Sens Actuators B 2010;147:741-7.

[46] Achatz DE, Meier RJ, Fischer LH, Wolfbeis OS. Luminescent sensing of oxygen using a quenchable probe and upconverting nanoparticles. Angew Chem Int Ed 2011;50:260-3.

[47] Hartmann P, Leiner MJ, Kohlbacher P. Photobleaching of a ruthenium complex in polymers used for oxygen optodes and its inhibition by singlet oxygen quenchers. Sens Actuators B 1998;51:196-202.

[48] Liu C, Lv X, Xing Y, Qiu J. Trifluoromethyl-substituted cyclometalated iridium^{III} emitters with high photostability for continuous oxygen sensing. J Mater Chem C 2015;3:8010-7.

[49] Amao Y, Ishikawa Y, Okura I. Green luminescent iridium(III) complex immobilized in fluoropolymer film as optical oxygen-sensing material. Anal Chim Acta 2001;445:177-82.

List of Tables:

Table 1 Photophysical and electrochemical data of the Ir(III) complexes.

Complexes	**λ_{abs} [a] (nm)**	**λ_{em} [b] (nm)**	**Φ_p [c]**	**τ [d] (μs)**	**E_{ox}^{onset} [e] (V)**	**E_g [f] [eV]**	**HOMO [g] (eV)**	**LUMO [g] (eV)[h]**	**CIE (x,y)**
Ir(ppy)$_2$(acac)[h]	260 (0.36), 340 (0.08), 412 (0.04), 460 (0.02)	518	0.34	1.55	0.71	2.54	-5.11	-2.57	0.25,0.67
Ir1	257 (0.55), 302 (0.51), 369 (0.46), 396 (0.42), 447 (0.10)	532	0.18	3.84	0.63	2.47	-5.03	-2.56	0.31,0.66
Ir2	258 (0.53), 304 (0.51), 361 (0.47), 445 (0.10)	530	0.29	3.90	0.58	2.49	-4.98	-2.49	0.30,0.66
Ir3	256 (0.71), 299 (0.69), 317 (0.70), 364 (0.63), 450 (0.13)	536	0.21	3.89	0.68	2.43	-5.08	-2.65	0.33,0.64
Ir4	249 (0.45), 278 (0.43), 293 (0.41), 419 (0.48), 472 (0.14)	558	0.30	3.46	0.77	2.36	-5.17	-2.81	0.42,0.57

[a] Measured in CH_2Cl_2 at a concentration of 10^{-5} M and extinction coefficients (10^5 $M^{-1}cm^{-1}$) are shown in parentheses. [b] The emission maximumin in degassed CH_2Cl_2 solution. [c] The quantum yields (Φ_p) in degassed CH_2Cl_2 solution were measured with [Ir(ppy)$_2$(acac)] (Φ_p= 0.34) as a standard (λ_{ex}= 400 nm). [d] Measured in degassed CH_2Cl_2 at a sample concentration of 10^{-5} M. [e] 0.1 M $[Bu_4N]PF_6$ in CH_2Cl_2, scan rate 100 mV s^{-1}, measured using saturated calomel electrode (SCE) as the standard. [f] E_g were calculated from the intersection of the normalized absorption and the emission spectra. [g] E_{HOMO} (eV) = -e(4.4 +E_{ox}^{onset}), E_{LUMO} (eV)= E_{HOMO} + E_g. [h] Reference 48. All measured at ambient temperature.

Table 2 Some of Ir(III) complexes used as oxygen sensing probes.

Probe	Support for immobilization	$\lambda_{ex}/_{em}$ (nm)	I_0/I_{100}	References
[Ir(ppy)$_2$(CN)$_2$]	nBuPTP	340/510	-	Chem Mater 2005;17:4765–73.
Ir(C$_{S-Me}$)$_2$(acac)	Polystyrene	475/566	-	Anal Chem 2007;79:7501–9.
N-833	Polystyrene	402/529	1.3	Talanta 2007;71:242–50.
N-926	Polystyrene	400/526	2.4	Talanta 2007;71:242–50.
Ir(ppy-NPh$_2$)$_3$	Ethyl cellulose	405/524	-	Chem Mater 2009;21,2173–5.
N969	AlOOH	350/490	47.6	Talanta 2010;82:620–6.
N969	Polystyrene	385/585	5.0	Talanta 2010;82:620–6.
Ir(mebtp)$_3$	FIB	296/595	7.41	Sens Actuators B 2010;145:278–84.
dye 3	AP200/19	335/470	-	Chem Mater 2012;24:2330−8.
Ir(piq)$_2$(acac)	ORMOSILs	-	-	Analyst 2013;138:1819–27.
Lx4	Ethyl cellulose	-	5.7	J Mater Chem C 2015;3:8010-7.
Ir(ppy)$_2$(acac)	Ethyl cellulose	400/517	5.8	This work
Ir1	Ethyl cellulose	400/528	16.2	This work
Ir2	Ethyl cellulose	400/528	16.4	This work
Ir3	Ethyl cellulose	400/534	15.2	This work
Ir4	Ethyl cellulose	400/557	14.1	This work

List of Scheme and Figures:

Scheme 1. Synthesis of bis-cyclometalated Ir(III) complexes for this study. (i) $Pd(OAc)_2$, K_2CO_3, $EtOH/H_2O$ 3:1(v/v), 80 ºC, in air, 30-60 min. (ii) $IrCl_3 \cdot 3H_2O$, $EtOCH_2CH_2OH/H_2O$ 3:1(v/v), 110 ºC, N_2, 24 h. (iii) Hacac, K_2CO_3, $EtOCH_2CH_2OH$, 120 ºC, N_2, 24 h.

Fig. 1. Absorption (up) and emission spectra (down, λ_{ex}= 400 nm) of **Ir1-Ir4** and $Ir(ppy)_2(acac)$ in CH_2Cl_2 solution at room temperature.

Fig. 2. Phosphorescence decay profiles of **Ir1-Ir4** and $Ir(ppy)_2(acac)$ in CH_2Cl_2 solution at room temperature.

Fig. 3. Illustration of simplified mechanism for oxygen sensing.

Fig. 4. (A) The transparent quartz plate (*r* = 7.0 mm) whose inner surface is covered with the oxygen sensing film. (B) SEM micrograph of the oxygen sensing film. (C) The diagram of the sensing layer.

Fig. 5. Photo-degradation histograms for the Ir(III) complexes/EC films under continuous illumination for 90 min at ambient atmospheric conditions.

Fig. 6. Stern-Volmer plots for oxygen sensing films of Ir(III) complexes immobilized in EC (intensity ratios I_0/I versus O_2 partial pressure).

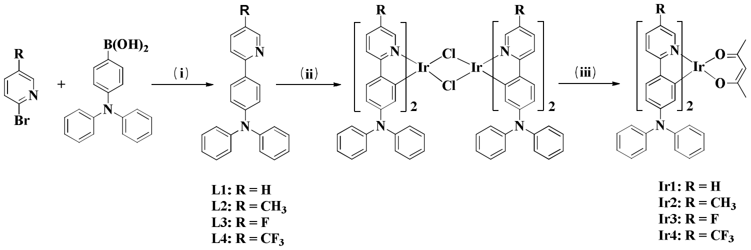

Scheme 1. Synthesis of bis-cyclometalated Ir(III) complexes for this study. (i) Pd(OAc)$_2$, K$_2$CO$_3$, EtOH/H$_2$O 3:1(v/v), 80 ºC, in air, 30-60 min. (ii) IrCl$_3$·3H$_2$O, EtOCH$_2$CH$_2$OH/H$_2$O 3:1(v/v), 110 ºC, N$_2$, h. (iii) Hacac, K$_2$CO$_3$, EtOCH$_2$CH$_2$OH, 120 ºC, N$_2$, 24 h.

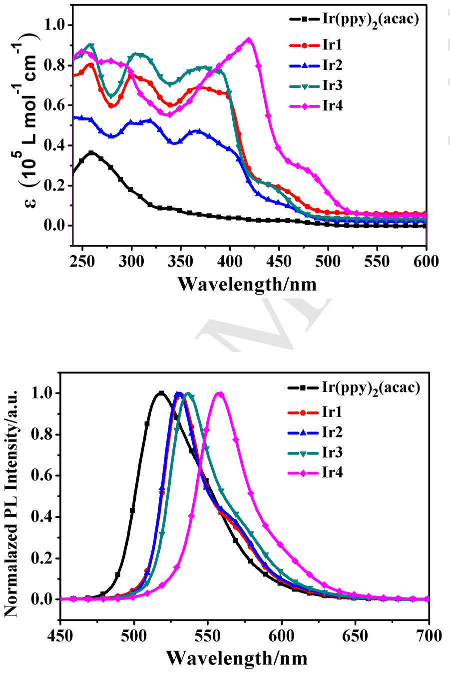

Fig. 1. Absorption (up) and emission spectra (down, λ_{ex}= 400 nm) of **Ir1-Ir4** and Ir(ppy)$_2$(acac) in CH$_2$Cl$_2$ solution at room temperature.

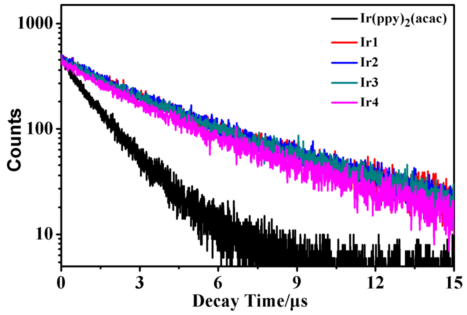

Fig. 2. Phosphorescence decay profiles of **Ir1-Ir4** and Ir(ppy)$_2$(acac) in CH$_2$Cl$_2$ solution at room temperature.

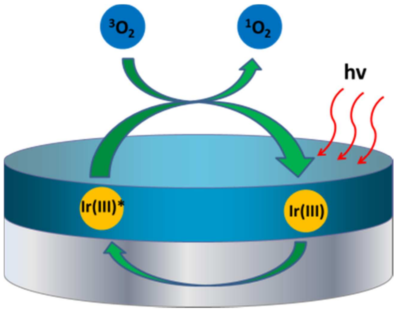

Fig. 3. Illustration of simplified mechanism for oxygen sensing.

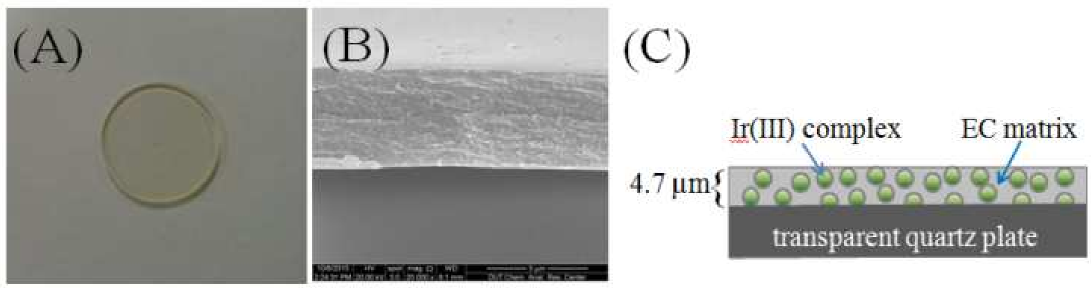

Fig. 4. (A) The transparent quartz plate (*r* = 7.0 mm) whose inner surface is covered with the oxygen sensing film. (B) SEM micrograph of the oxygen sensing film. (C) The diagram of the sensing layer.

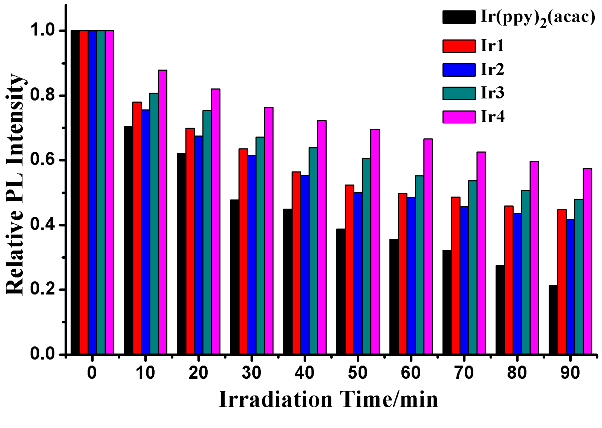

Fig. 5. Photo-degradation histograms for the Ir(III) complexes/EC films under continuous illumination for 90 min at ambient atmospheric conditions.

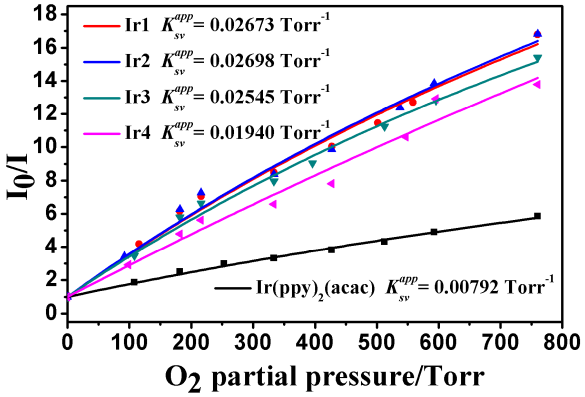

Fig. 6. Stern-Volmer plots for oxygen sensing films of Ir(III) complexes immobilized in EC (intensity ratios I_0/I versus O_2 partial pressure).

Research highlights

1) A series of NPh_2-modified Ir(III) complexes **Ir1-Ir4** have been synthesized.
2) The luminescent lifetimes of **Ir1-Ir4** are prolonged due to the diphenylamino group.
3) The photostabilities of **Ir1-Ir4** are enhanced efficiently over $Ir(ppy)_2(acac)$.
4) **Ir1-Ir4** demonstrated excellent oxygen sensitivity with $I_0/I_{100} > 14$.